Sub-Doppler High-Resolution Excitation Spectroscopy of Dibenzo-*p*-dioxin

Masaaki Baba*

Department of Chemistry, Graduate School of Science, Kyoto University, Kyoto 606-8501, Japan

Atsushi Doi, Yoshio Tatamitani, Shunji Kasahara, and Hajime Katô

Molecular Photoscience Research Center, Kobe University, Nada-ku, Kobe 657-8501, Japan

Received: October 28, 2003; In Final Form: December 14, 2003

Sub-Doppler high-resolution excitation spectra of dibenzo-*p*-dioxin (DD) have been observed for the 0_0^0 and $0_0^0 + 22$ cm^{-1} bands of the $S_1 \leftarrow S_0$ transition by crossing a tunable laser beam perpendicular to a collimated molecular beam. The spectrum was composed of several strong *Q* lines at the band center and *P* and *R* lines on both sides. The rotational constants of the $S_0(v'' = 0)$, $S_1(v' = 0)$, and $S_1(v' = 0 + 22$ cm$^{-1})$ states were determined by analysis of the observed rotational contours. The observed spectra were reproduced well by simulating the spectra as the *a*-type transition, whose transition moment is parallel to the long axis of the molecule. Accordingly, the S_1 state is identified to be a $^1B_{1u}$ state. From the rotational constants, the DD molecule has been shown to be planar in the S_0 state and folded slightly out-of-plane (butterfly form) in the S_1 state: the dihedral angles of the phenyl ring are 170.6° and 173.4° in the $S_1(v' = 0)$ and $S_1(v' = 0 + 22$ cm$^{-1})$ states, respectively. The $0_0^0 + 22$ cm^{-1} band is assigned as a transition to the a_g component of the butterfly mode. The line widths were much larger than the instrumental resolution, and the lifetime of the S_1 state was evaluated to be ∼500 ps.

Introduction

Polychlorinated dibenzo-*p*-dioxins (PCDDs) are highly toxic, and the toxic equivalency factors (TEFs) have been defined for various congeners.[1] To investigate and remove the toxicity, it is important to study the molecular structure and fundamental properties. Dibenzo-*p*-dioxin (DD, the structure of which is shown in Figure 1) is one of the prototype molecules of dioxins for which there have been many spectroscopic studies.[2−8] The vibrational structure of the $S_1 \leftarrow S_0$ transition has been observed by multiphoton ionization detection in a supersonic jet,[4,5] and it was suggested that the configuration of the DD molecule in the S_1 and S_0 states are different: the molecule has a "butterfly" configuration in the S_0 state and becomes flatter in the S_1 state. The molecular structure in the S_0 state is approximately planar in a single crystal, according to X-ray diffraction (XRD) analysis.[9,10] Gastilovich et al.[8] concluded that the molecule is planar in both the S_0 and S_1 states (D_{2h} symmetry), through analysis of the IR and Raman spectra of the DD molecule in the condensed phase. They also suggested that the S_1 state has *g*-type symmetry, on the basis that the intensity of the 0_0^0 band is weak and the intensity of the $0_0^0 + 22$ cm^{-1} band (*u*-type vibration of the butterfly mode) is stronger than the 0_0^0 band. More extensive studies are necessary to determine the molecular geometry and the electronic state of the DD molecule.

High-resolution spectroscopy is very powerful to study the geometrical structure, electronic structure, direction of the transition moment, vibrational and rotational energy levels, and potential energy surfaces. We observed sub-Doppler high-resolution excitation spectra of the DD molecule by crossing a tunable laser beam perpendicular to a collimated molecular beam. This technique has been applied successfully to several molecules.[11,12] The results and the analysis are reported in this article, and the molecular geometry and the electronic structure in the S_0 and S_1 states are studied.

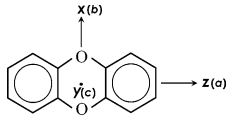

Figure 1. Structure of dibenzo-*p*-dioxin (DD) and the coordinate axes.

Departing from the choice of coordinate axes that were selected by Gastilovich et al.[2] and Zimmermann et al.,[5] we chose the top axis (*a*-axis) as the molecule-fixed *z*-axis and the *x*-axis parallel to the O−O axis (*b*-axis). In a butterfly form of C_{2v} symmetry, the *y*-axis is the 2-fold C_2-axis. Characters and species of point groups D_{2h} and C_{2v} and the correlation of species in the present choice of coordinates are listed in Table 1. In D_{2h} symmetry, the conversion from Gastilovich et al.'s convention $x, y, z, a_g, b_{1g}, b_{2g}, b_{3g}, a_u, b_{1u}, b_{2u}, b_{3u}$ to the present convention is $y, z, x, a_g, b_{3g}, b_{1g}, b_{2g}, a_u, b_{3u}, b_{1u}, b_{2u}$, respectively.

Experimental Section

Dibenzo-*p*-dioxin (Wako Chemical) was heated to 150 °C in a stainless-steel container. The vapor was mixed with argon gas and expanded into a vacuum chamber through a pulsed nozzle (with an orifice diameter of 0.8 mm). The molecular beam was collimated with a skimmer and differential pumping. The distance between the nozzle and skimmer was 25 mm, and the skimmer diameter was 1 mm. The residual Doppler width is evaluated to be ∼0.001 cm^{-1} in this arrangement. A single-mode tunable ring dye laser (Coherent, model CR699-29, Rhodamine 6G dye) pumped by a Nd:YVO_4 laser (Coherent,

* Author to whom correspondence should be addressed. E-mail: baba@kuchem.kyoto-u.ac.jp.

10.1021/jp037246l CCC: $27.50
Published on Web 01/22/2004

TABLE 1: Character Tables of Point Groups D_{2h} and C_{2v} in the Present Choice of the Coordinates for the DD Molecule, and the Correlation of Symmetry Species

D_{2h}	E	$C_2(z)$	$C_2(y)$	$C_2(x)$	i	$\sigma(xy)$	$\sigma(xz)$	$\sigma(yz)$		C_{2v}[a]
A_g	1	1	1	1	1	1	1	1		A_1
B_{1g}	1	1	−1	−1	1	1	−1	−1	R_z	B_1
B_{2g}	1	−1	1	−1	1	−1	1	−1	R_y	A_2
B_{3g}	1	−1	−1	1	1	−1	−1	1	R_x	B_2
A_u	1	1	1	1	−1	−1	−1	−1		A_2
B_{1u}	1	1	−1	−1	−1	−1	1	1	z	B_2
B_{2u}	1	−1	1	−1	−1	1	−1	1	y	A_1
B_{3u}	1	−1	−1	1	−1	1	1	−1	x	B_1

C_{2v}	E	$C_2(y)$	$\sigma(xy)$	$\sigma(yz)$	
A_1	1	1	1	1	y
A_2	1	1	−1	−1	R_y
B_1	1	−1	1	−1	x, R_z
B_2	1	−1	−1	1	z, R_x

[a] Correlation of symmetry species.

model Verdi V10) was used as a light source. The UV light was obtained by the second harmonic generation, using an enhancement external cavity (Spectra Physics, model Wavetrain-SC) that was equipped with a BaB_2O_4 crystal. The power of the UV light was 20 mW, and the line width was 0.0003 cm^{-1}. Fluorescence was collected and focused to a photomutiplier tube (Hamamatsu, model R585) by a lens through a color filter (Toshiba, model UV33) to block the scattered laser light. The output of the photomultiplier was processed by a photon counter (Stanford Research, model SR 400). The fluorescence excitation spectrum was obtained by recording the photon number as a function of the wavenumber of the scanning laser light. A portion of the output of the ring dye laser was phase-modulated at 30 MHz by an electro-optic modulator and was passed through an Etalon (Burleigh, model CFT-500, FSR = 150 MHz, finesse = 30). The cavity length was stabilized against a single-mode Nd:YAG laser (InnoLight, model Prometheus 20), whose frequency was locked to one of the hyperfine lines of the iodine molecule. The frequency marks were recorded by detecting the intensity of transmitted light. The Doppler-free saturation spectrum of the iodine molecule was also measured simultaneously, and the absolute wavenumbers of the frequency marks were calibrated with an accuracy of better than 0.0002 cm^{-1} by referring to the Doppler-free high-resolution spectral atlas of the iodine molecule.[13]

Results and Discussion

The sub-Doppler high-resolution excitation spectrum of the 0_0^0 band is shown in Figure 2a. The several strong peaks of the Q lines are observed at the band center. The P and R lines are observed at the low- and high-energy sides of the Q lines, respectively. A series of peaks with a line width of ∼0.01 cm^{-1} and a spacing of ∼0.03 cm^{-1} are observed on both sides of the Q lines. The spectrum of the vibrational band 0_0^0 + 22 cm^{-1}, which is observed at an energy of 22 cm^{-1} higher than that of the 0_0^0 band, is shown in Figure 3a. The intensity of the 0_0^0 + 22 cm^{-1} band is several times stronger than that of the 0_0^0 band; however, the profile of the spectrum is very similar.

Although the instrumental resolution is much higher than the observed line widths, the rotational lines were not fully resolved, and therefore the spectra were analyzed by calculating the rotational contour. Nonzero matrix elements of the A-reduced

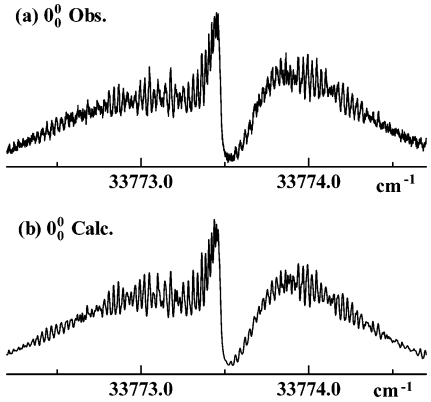

Figure 2. The 0_0^0 band of the $S_1 \leftarrow S_0$ transition of the DD molecule: (a) the observed sub-Doppler fluorescence excitation spectrum and (b) the simulated sub-Doppler fluorescence excitation spectrum.

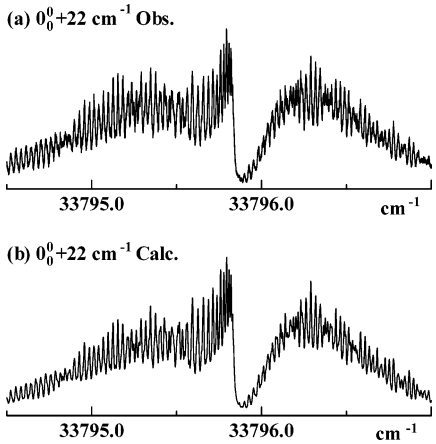

Figure 3. The 0_0^0 + 22 cm^{-1} band of the $S_1 \leftarrow S_0$ transition of the DD molecule: (a) the observed sub-Doppler fluorescence excitation spectrum and (b) the simulated sub-Doppler fluorescence excitation spectrum.

Hamiltonian for a near prolate symmetric-top molecule are given by[14]

$$\langle JKM|H_r^{(A)}|JKM\rangle = T_0 + \frac{1}{2}(B+C)J(J+1) + \left[A - \frac{1}{2}(B+C)\right]K^2 - \Delta_J J^2(J+1)^2 \quad (1)$$

$$\langle JK \pm 2M|H_r^{(A)}|JKM\rangle = \frac{1}{4}(B-C)\{[J(J+1) - K(K\pm 1)][J(J+1) - (K\pm 1)(K\pm 2)]\}^{1/2} \quad (2)$$

where $|JKM\rangle$ is the eigenfunction of a symmetric-top molecule, J is the quantum number of the total angular momentum $\boldsymbol{J}$, K and M are the quantum numbers of the projection of $\boldsymbol{J}$ along the molecule-fixed z-axis and the space-fixed Z-axis, respectively, and the A, B, and C are the rigid rotor rotational constants, and Δ_J is the symmetric-top quartic centrifugal distortion constant. To fit the molecular constants to the observed transition energies and to calculate the rotational contour, we have used the AsyrotWin program.[15]

By referencing the XRD data of the DD molecule,[9,10] the two C_6H_4 moieties were fixed as the distances R(C−C) = 1.39 Å, R(C−H) = 1.08 Å, and the angles ∠C−C−C = ∠C−C−H = 120°. If we assume that the DD molecule is planar, ∠C−O−C = 116°, and R(C−O) = 1.378 Å, the rotational constants are A = 0.07179 cm^{-1}, B = 0.01599 cm^{-1}, and C = 0.01308 cm^{-1}. If we assume that the DD molecule has a "butterfly"

TABLE 2: Molecular Constants of the S_0 $^1A_g(v'' = 0)$, S_1 $^1B_{1u}(v' = 0)$, and S_1 $^1B_{1u}(v' = 0 + 22\ cm^{-1})$ States

	$S_0\ ^1A_g(v'' = 0)$	$S_1\ ^1B_{1u}(v' = 0)$	$S_1\ ^1B_{1u}(v' = 0 + 22\ cm^{-1})$
rotational constants			
A	0.071343(182)[a]	0.070167(182)	0.070088(182)
B	0.016060(10)	0.016077(10)	0.016051(10)
C	0.013109(10)	0.013123(10)	0.013081(10)
symmetric-top quartic centrifugal distortion constant, Δ_J	$7(1) \times 10^{-9}$	$7(1) \times 10^{-9}$	$7.5(5) \times 10^{-9}$
band origin, T_0		33773.4780(5)	33795.8415(5)
line width, Γ (cm^{-1})		0.011(1)	0.007(1)
moments of inertia (10^{-46} kg m^2)			
I_a	39.237	39.894	39.939
I_b	174.30	174.12	174.40
I_c	213.54	213.31	214.00
inertial defect, Δ (10^{-46} kg m^2)	0.0(1)	−0.70	−0.34

[a] This value was obtained by assuming a planar structure: $1/C = 1/A + 1/B$. The error in *A* is estimated as the inertial defect, which arises by zero-point motions, is ±0.1.

configuration and the dihedral angle is 164°, which was estimated from the electric dipole moment,[16] the rotational constants are $A = 0.06998\ cm^{-1}$, $B = 0.01621\ cm^{-1}$, and $C = 0.01329\ cm^{-1}$. From the spacing of the *P* and *R* lines, two bands that are shown in Figures 2 and 3 can be identified as *a*-type bands: the transition moment is along the *a*-axis, and the transitions are allowed for $\Delta J = \pm 1, 0$ and $\Delta K = 0$.[17] Therefore, the symmetry species of the S_1 state of the excited level is identified as B_{1u}.

The strong lines at the band center are the ^qQ lines ($\Delta J = 0$ and $\Delta K = 0$). The peaks are shifted to the lower energy side as *K* increases, and it suggests that the value of $A - {}^1/_2(B + C)$ in the S_1 state is smaller than that in the S_0 state. The H atom has the nuclear spin ($I = {}^1/_2$), and the relative populations in the ground state are 76:60:60:60 for the *ee*:*eo*:*oe*:*oo* levels. By taking the nuclear statistics into consideration, we calculated the rotational contour by changing the rotational constants, the spectral width of rotational line, and population on rotational levels in the molecular beam.

The prominent lines in the spectrum are regular; however, there are several irregular parts. Each feature is composed of several transitions, and the rotational contour is very sensitive to the magnitudes of rotational constants. The rotational constants are iteratively fitted to reproduce the observed rotational contour. The observed and simulated spectra of the 0_0^0 and $0_0^0 + 22\ cm^{-1}$ bands are shown in Figures 2 and 3, respectively. More detail is shown in Figure 4 for a portion of the 0_0^0 and $0_0^0 + 22\ cm^{-1}$ bands. The population for the rotational levels in the S_0 state, which was used in the fit, is shown in Figure 4c: the rotational temperature is ~10 K. From the fit of the *P* and *R* lines, the molecular constants *B* and *C* could be determined, in both the ground and excited states. Because only the $\Delta K = 0$ transitions were observed, only the difference $A' - A''$ could be determined from the fit, where the prime and double prime symbols denote the upper and lower states, respectively. The molecular constants B'' and C'' in the ground state are close to the values of a planar structure. For a planar molecule, the relation $1/C = 1/A + 1/B$ holds.[18] The values of A'' were determined using this relation. The resulting molecular constants are listed in Table 2. The line widths were determined from the fit and also are listed in Table 2. This width is much larger than the instrumental resolution. The line width is dominated by the lifetime of the excited level, and the lifetime of the $S_1(v = 0)$ levels is evaluated to be ~500 ps.

The A' value is smaller than A'', and the inertial defect Δ is not zero in the S_1 $^1B_{1u}$ state (see Table 2). It indicates that the molecule is nonplanar in the S_1 $^1B_{1u}$ state. By fixing the two

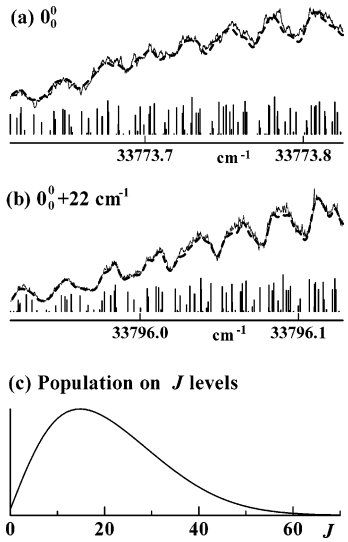

Figure 4. A portion of the observed spectrum (full line) and the simulated rotational contour (broken line), whose components of transition lines are shown by vertical bars ((a) the 33773.615−33773.825 cm^{-1} region of the 0_0^0 band and (b) the 33795.918−33796.128 cm^{-1} region of the $0_0^0 + 22\ cm^{-1}$ band). Population on *J* levels in the S_0 $^1A_g(v = 0)$ state used to calculate the rotational contours is shown in Figure 4c.

C_6H_4 moieties as R(C−C) = 1.39 Å, R(C−H) = 1.08 Å, and ∠C−C−C = ∠C−C−H = 120°, the three parameters R(C−O), ∠C−O−C, and the dihedral angle of the phenyl ring were determined to be 1.396 Å, 112.9°, and 170.6°, respectively, for the $S_1(v = 0)$ state, and 1.403 Å, 112.2°, and 173.4°, respectively, for the $S_1(v = 0 + 22\ cm^{-1})$ state by fitting to the rotational constants listed in Table 2.

A theoretical ab initio calculation using the B3LYP method on the conformation of the DD molecule has been reported recently,[19] and the optimized geometry was calculated to be planar and had D_{2h} symmetry for the S_0 state. We performed the calculation at the B3LYP/6-311G(d,p) level and confirmed their results, and the rotational constants in the S_0 ^1A_g state were calculated to be $A'' = 0.07151\ cm^{-1}$, $B'' = 0.01595\ cm^{-1}$, and $C'' = 0.01304\ cm^{-1}$. These values are similar to the experimentally obtained values (see Table 2). The frequencies of the normal vibrations were also calculated, and the vibration of the lowest frequency was a butterfly mode (the symmetry species is b_{2u} in a planar structure and a_1 in a bent structure) and the frequency was 35 cm^{-1}.

The transition energies (ΔE) and oscillator strengths (*f*) for lower excited states were calculated using the RCIS method

TABLE 3: Excitation Energy and Oscillator Strength for Transitions to the Lower Six States, Calculated by the RCIS Method for the Molecular Configuration Optimized in the S_0 ^1A_g State at the B3LYP/6-311G(d,p) Level

state	wave function[a]	excitation energy, ΔE (cm^{-1})	oscillator strength, f
1^1B_{2g}	0.601| 48, 49| − 0.220| 47, 51| + 0.194| 46, 52| − 0.179| 45, 50|	45294	0.000
1^1B_{1u}	0.506| 48, 51| + 0.323| 47, 49| + 0.308| 46, 50| + 0.199| 45, 52|	47592	0.096
2^1A_g	0.533| 48, 50| + 0.237| 47, 52| + 0.262| 46, 51| + 0.294| 45, 49|	47693	0.000
1^1B_{3u}	−0.321| 48, 52| + 0.420| 47, 50| − 0.309| 46, 49| + 0.321| 45, 51|	51836	0.011
2^1B_{2g}	0.302| 48, 49| + 0.451| 47, 51| + 0.404| 45, 50| + 0.105| 43, 49|	60068	0.000
2^1B_{1u}	−0.388| 48, 51| + 0.524| 47, 49| + 0.223| 45, 52|	60719	2.305

[a] $|i, j|$ represents an antisymmetrized wave function of the state where an electron is moved from molecular orbital i to molecular orbital j, from the electronic configuration in the ground state S_0 ^1A_g.

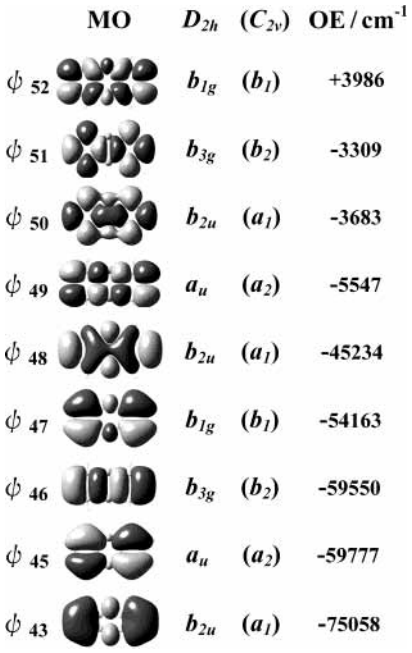

Figure 5. Molecular orbitals ψ_i around the highest occupied molecular orbital (HOMO) ψ_{48} and the lowest unoccupied molecular orbital (LUMO) ψ_{49} obtained by ab initio calculations at the B3LYP/6-311G-(d,p) level for the molecular configuration optimized in the ground state. The dark and light components correspond to different signs of the orbitals. The symmetry species in the D_{2h} (C_{2v}) symmetry, and the orbital energies (in units of cm^{-1}) are also indicated.

for the molecular configuration optimized in the ground state at the B3LYP/6-311G(d,p) level, and the results are listed in Table 3. The molecular orbitals around the highest occupied molecular orbital (HOMO) and lowest unoccupied molecular orbital (LUMO), and the orbital energies, are shown in Figure 5. The lowest allowed transition is $1^1B_{1u} \leftarrow 1^1A_g$, and the transition moment is along the *z*-axis. Therefore, this transition is identified as the $S_1 \leftarrow S_0$ transition. The calculated oscillator strength of the $1^1B_{1u} \leftarrow 1^1A_g$ transition is much smaller than that of the $2^1B_{1u} \leftarrow 1^1A_g$ transition, and this is consistent with the observed weak intensity of the $S_1 \leftarrow S_0$ transition. The energy of the S_1 $^1B_{1u} \leftarrow S_0$ ^1A_g transition was calculated to be 47 600 cm^{-1}, which is much larger than the observed energy. The optimized molecular structure for the 1^1B_{1u} state was calculated to be planar, and it is different from the observed results. A more-accurate calculation for the excited state is necessary to reproduce the observed results.

The intensity of the $0_0^0 + 22$ cm^{-1} band was several times stronger than that of the 0_0^0 band. This fact can be explained as follows. The DD molecule is planar in the $S_0(v'' = 0)$ state and bent in both the $S_1(v' = 0)$ and $S_1(v' = 0 + 22$ $cm^{-1})$ states, as we can see from the rotational constants. The levels $v' = 0$ and $v' = 0 + 22$ cm^{-1} in the S_1 state lie below the potential barrier to inversion of the butterfly mode. The wave functions of the identical sets of vibrational levels start to overlap by the penetration as the levels approach to the top of the potential barrier. The dihedral angle of the phenyl ring in the $S_1(v' = 0 + 22$ $cm^{-1})$ state is evaluated to be 173.4°, and it is 170.6° in the $S_1(v' = 0)$ state. Accordingly, the potential barrier would be low enough for the penetration of wave functions of the butterfly mode. The wave functions of each pair of butterfly mode a_1 in C_{2v} symmetry overlap either with the signs in-phase or out-of-phase. The resulting wave functions are either a_g or b_{2u} symmetry in the D_{2h} point group. An electric dipole transition to the a_g component of the butterfly mode is allowed from the S_0 $^1A_g(v'' = 0)$ state, and the transition moment is along the *a*-axis. The Franck−Condon factor $|\langle v'' = 0|v' = 1(a_g$: butterfly)$\rangle|^2$ is larger than $|\langle v'' = 0|v' = 0(a_g$: butterfly)$\rangle|^2$ when the DD molecule is planar in the $S_0(v'' = 0)$ state. The transition strength increases as a vibrational level approaches the top of the potential barrier.[18]

The increase in strength of the transition to the $v' = 1$ level of the a_g component can also occur by Herzberg−Teller coupling with the 2^1B_{1u} state, because the oscillator strength of the $2^1B_{1u} \leftarrow 1^1A_g$ transition is much larger than that of the $1^1B_{1u} \leftarrow 1^1A_g$ transition (see Table 3). The increase in strength of the vibronic band in the b_{2u} component of the butterfly mode would be offset by Herzberg−Teller coupling with an $^1B_{3g}$ state, which is forbidden in D_{2h} but allowed in C_{2v} symmetry. However, these may be of minor contribution, because the S_1 $^1B_{1u}(v' = 0) \leftarrow S_0$ $^1A_g(v'' = 0)$ transition is an allowed transition.

In summary, Sub-Doppler high-resolution spectra of dibenzo-*p*-dioxin (DD) have been observed for the 0_0^0 and $0_0^0 + 22$ cm^{-1} bands of the $S_1 \leftarrow S_0$ transition by crossing a tunable laser beam perpendicular to a collimated molecular beam. From the analysis of the rotational contours, the molecular constants of the $S_0(v'' = 0)$, $S_1(v' = 0)$, and $S_1(v' = 0 + 22$ $cm^{-1})$ levels were determined. Both of the 0_0^0 and $0_0^0 + 22$ cm^{-1} bands were the *a*-type, and, therefore, the direction of the transition moments is parallel to the top axis. The symmetry of the S_1 state is accordingly identified as B_{1u}. From the rotational constants, it is determined that the DD molecule is planar in the S_0 state and is folded slightly out-of-plane (butterfly form) in the S_1 state: the dihedral angle of the phenyl ring is evaluated to be 170.6° for the $S_1(v' = 0)$ level and 173.4° for the $S_1(v' = 0 + 22$ $cm^{-1})$ level. The $S_1(v' = 0 + 22$ $cm^{-1})$ level is identified as the $S_1(v' = 1$: a_g component of butterfly mode) level. An electric dipole transition to the a_g component of the butterfly mode from the S_0 $^1A_g(v'' = 0)$ state is allowed by the tunnel effect through the potential barrier to inversion of the butterfly mode. The Franck−Condon factor $|\langle v'' = 0|\ v' = 1(a_g$: butterfly)$\rangle|^2$ is larger than $|\langle v'' = 0|v' = 0(a_g$: butterfly)$\rangle|^2$ in the S_1 $^1B_{1u}$(bent) $\leftarrow S_0$ ^1A_g(planar) electronic transition, and the transition moment is along the *a*-axis. These findings are consistent with the observed results. The lifetime of the excited state was found to be shorter

than the radiative lifetime from the line width, and it would be originating from the predissociation. The toxicity of the PCDDs may be removed by irradiating light of an appropriate wavenumber.

Acknowledgment. This work is supported by a JSPS research grant for Future Program: Photoscience and a Grant-in-Aid for Scientific Research from the Ministry of Education, Culture, Sports, Science, and Technology of Japan.

References and Notes

(1) Van den Berg, M., et al. *Environ. Health Perspect.* **1998**, *106*, 775.
(2) Gastilovich, E. A.; Klimenko, V. G.; Korol'kova, N. V.; Nurmukhametov, R. N. *Russ. Chem. Rev.* **2000**, *69*, 1037.
(3) Funk, D. J.; Oldenborg, R. C.; Dayton, D.-P.; Lacosse, J. P.; Draves, J. A.; Logan, T. J. *Appl. Spectrosc.* **1995**, *49*, 105.
(4) Weickhardt, C.; Zimmermann, R.; Boesl, U.; Schlag, E. W. *Rapid Commun. Mass Spectrom.* **1993**, *7*, 183.
(5) Zimmermann, R.; Boesl, U.; Lenoir, D.; Kettrup, A.; Grebner, Th. L.; Neusser, H. J. *Int. J. Mass Spectrom. Ion Process.* **1995**, *145*, 97.
(6) Klimenko, V. G.; Nurmukhametov, R. N.; Gastilovich, E. A. *Opt. Spectrosc.* **1997**, *83*, 84.
(7) Klimenko, V. G.; Nurmukhametov, R. N.; Gastilovich, E. A.; Lebedev, S. A. *Opt. Spectrosc.* **2000**, *88*, 339.
(8) Gastilovich, E. A.; Klimenko, V. G.; Korol'kova, N. V.; Nurmukhametov, R. N. *Chem. Phys.* **2002**, *282*, 265.
(9) Senma, M.; Taira, Z.; Taga, T.; Osaki, K. *Cryst. Struct. Commun.* **1973**, *2*, 311.
(10) Singh, P.; McKinney, J. D. *Acta Crystallogr., Sect. B: Struct. Crystallogr. Cryst. Chem.* **1978**, *B34*, 2956.
(11) Majewski, W.; Meerts, W. L. *J. Mol. Spectrosc.* **1984**, *104*, 271.
(12) Pratt, D. W. *Annu. Rev. Phys. Chem.* **1998**, *49*, 481.
(13) Katô, H., et al. *Doppler-Free High-Resolution Spectral Atlas of Iodine Molecule 15000 to 19000 cm^{-1}*; JSPS: Tokyo, 2000.
(14) Watson, J. K. G. *Vibrational Spectra and Structure, A Series of Advance*; Durig, J. R., Ed.; Marcel Dekker: New York, 1977; Vol. VI, pp 1−89.
(15) Judge, R. H.; Clouthier, D. J. *Comput. Phys. Commun.* **2001**, *135*, 293.
(16) Colonna, F. P.; Distefano, G.; Galasso, V.; Irgolic, K. J.; King, C. E.; Pappalardo, G. C. *J. Organomet. Chem.* **1978**, *146*, 235.
(17) Herzberg, G. *Molecular Spectra and Molecular Structure, III. Electronic Spectra and Electronic Structure of Polyatomic Molecules*; Van Nostrand Reinhold: New York, 1966.
(18) Herzberg, G. *Molecular Spectra and Molecular Structure, II. Infrared and Raman Spectra of Polyatomic Molecules*; Van Nostrand Reinhold: New York, 1945.
(19) Kim, S.; Kwon, Y.; Lee, J.; Choi, S.; Choo, J. *J. Mol. Struct.* **2003**, *655*, 451.